



LAWRENCE
LIVERMORE
NATIONAL
LABORATORY

Design of a Vestibular Prosthesis for Sensation of Gravito-inertial Acceleration

K. N. Hageman, M. R. Chow, P. J. Boutros, D. Roberts,
A. C. Tooker, K. Y. Lee, S. H. Felix, S. S. Pannu, C. C.
Della Santina

November 5, 2015

ASME Design of Medical Devices
Minneapolis, MN, United States
April 11, 2016 through April 14, 2016

Disclaimer

This document was prepared as an account of work sponsored by an agency of the United States government. Neither the United States government nor Lawrence Livermore National Security, LLC, nor any of their employees makes any warranty, expressed or implied, or assumes any legal liability or responsibility for the accuracy, completeness, or usefulness of any information, apparatus, product, or process disclosed, or represents that its use would not infringe privately owned rights. Reference herein to any specific commercial product, process, or service by trade name, trademark, manufacturer, or otherwise does not necessarily constitute or imply its endorsement, recommendation, or favoring by the United States government or Lawrence Livermore National Security, LLC. The views and opinions of authors expressed herein do not necessarily state or reflect those of the United States government or Lawrence Livermore National Security, LLC, and shall not be used for advertising or product endorsement purposes.

Design of a Vestibular Prosthesis for Sensation of Gravito-inertial Acceleration

Kristin N. Hageman¹, Margaret R. Chow¹, Peter J. Boutros¹, Dale Roberts², Angela Tooker³, Kye Lee³, Sarah Felix³, Satinderpall S. Pannu³, Charles C. Della Santina^{1,2}

¹Department of Biomedical Engineering, Johns Hopkins School of Medicine

²Department of Otolaryngology Head & Neck Surgery, Johns Hopkins School of Medicine

³Lawrence Livermore National Laboratory

1 Background

The vestibular system of the inner ear acts as a six degree of freedom (DOF) motion sensor of head rotational velocity and gravito-inertial acceleration (GIA), the latter being the sum of acceleration due to gravity and linear/translational head movement. There are two classes of sensors in the ear: three mutually orthogonal rotation sensors (semicircular canals, SCCs) and two GIA sensors (utricle and saccule, collectively called the otolith end organs). Each of the inner ear's 5 inertial sensors encodes motion using pulse frequency modulation (PFM) of the afferent neuron firing rates above and below naturally nonzero spontaneous activity rates [1].

Sensation of head motion drives ocular, postural and autonomic reflexes that help maintain steady vision, stable gait and balance. Individuals with profound loss of vestibular sensation, termed bilateral vestibular deficiency (BVD), suffer reduced quality of life due to poor visual acuity during head movement, illusory motion of visible objects during head movements, postural instability and chronic disequilibrium. There is no adequate treatment for chronic BVD unresponsive to rehabilitation [1]. This is in marked contrast to the case of deafness, for which cochlear implants (CI) are remarkably successful at restoring at least a partial sense of hearing.

Inspired by the success of CIs, multiple groups are working toward development of vestibular prostheses designed to sense head motion and electrically stimulate branches of the vestibular nerve ([2] for review). Research toward a vestibular prosthesis has focused on stimulation of the SCCs [3–6]; however, to more completely restore vestibular reflexes, stimulation of the otolith end organs is essential. Extending the existing Johns Hopkins multichannel vestibular prosthesis (MVP) to stimulate the otolith end organs poses several engineering and physiologic/anatomic challenges. The existing MVP architecture (black in Fig. 1) relies on an off-the-shelf commercial 3DOF gyroscope for sensation of head velocities and uses a microcontroller to convert sensed signals into a PFM train of charge-balanced, biphasic pulses based on a programmable velocity-to-pulse rate map. Stimulus pulse frequency is typically set near the spontaneous firing rate of vestibular afferent neurons and modulates to encode head movement [4]. To encode changes in GIA, additional components are required (red in Fig. 1).

Recent development of an application specific integrated

circuit (ASIC) [7] increased the number of electrode outputs. The work presented here aimed (1) to design and fabricate electrode arrays suited to otolith end organs and (2) to expand the capabilities of the MVP to encode GIA accelerations.

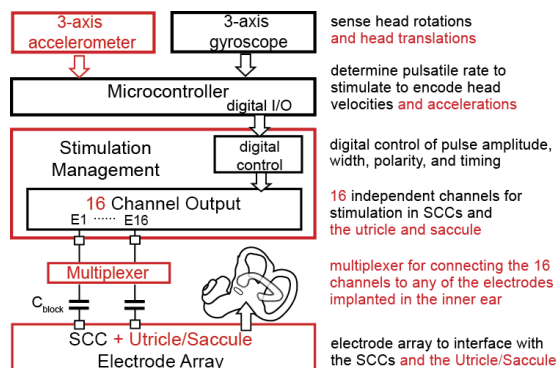


Figure 1. Johns Hopkins Vestibular NeuroEngineering Lab Multichannel Vestibular Prosthesis (MVP) architecture. Black boxes indicate the pre-existing framework of the MVP [4]. Red indicates what must be added to restore utricle/saccule function.

2 Methods

We designed electrode arrays for stimulation of chinchilla utricle and saccule based on a 3D anatomic model derived from reconstructed chinchilla micro-CT scans (Fig. 2A) [8].

Thin-film polyimide electrodes were micro-fabricated with multiple layers of trace metal insulated with interleaved layers of polyimide. To maximize the number of electrode contacts, electrode size was kept to the minimal that remained within safe charge injection limits. The 101 μm diameter electrode contacts (Fig. 2B) were designed using electrochemically activated iridium oxide film (AIROF), offering significant increase in safe charge injection at the electrode/saline interface (max 1200 $\mu\text{C}/\text{cm}^2$) compared to equal area bare platinum electrodes (max 24 $\mu\text{C}/\text{cm}^2$) [9].

Electrodes were tested in 0.9% NaCl saline using 50 μA -1 mA, 25-100 μs /phase biphasic, charge-balanced, cathodic-first current pulses.

In the new MVP system incorporating GIA sensation, a motion processing unit (Invensense MPU9250) senses angular velocities and linear acceleration. The new firmware maps velocity-to-pulse rates [4] and also includes a mapping for acceleration-to-pulse rate [10]. To test this mapping, the motion sensor was mounted onto a Moog 6DOF2000E motion

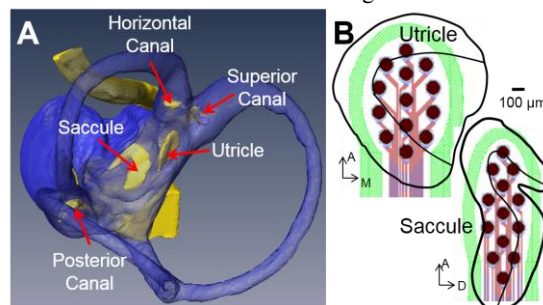


Figure 2. A. 3D reconstruction of chinchilla vestibular labyrinth [8]. Blue: fluid spaces of the inner ear; yellow: nerve and neurosensory epithelia, which are the targets for prosthetic stimulation. B. The electrode designs based on the geometry of the otolith end organs (outlines from [11]). Green: edge of the electrode array.

platform. The prosthesis was programmed for velocity-to-pulse rate on one “SCC-intended” electrode and acceleration-to-pulse rate on one “otolith-intended” electrode. The motion platform delivered lateral (left-right) sinusoidal accelerations at 2 Hz, 2 m/s² peak acceleration, followed by a 2 Hz, 20°/s peak velocity, and finally a combination of rotation and translation. Instantaneous velocity, acceleration, and pulse rates on both electrodes were recorded for analysis.

3 Results

Micromachining polyimide electrode arrays yields a large number of electrodes while maintaining small size, flexibility, and precisely defined geometry. The electrode array shown in Fig. 3A comprises 50 AIROF electrode contacts: 13 for utricle, 13 for saccule, and 8 for each of 3 SCCs. The 50 AIROF electrodes from one representative array have an average impedance of 5.75 ± 0.84 kOhms at 1.194 kHz. While maintaining AIROF safe charge injection ($1200 \mu\text{C}/\text{cm}^2$), current pulses up to 960 μA at 100 μs /phase can be delivered with a compliance voltage under 11 V. Example voltage waveforms recorded during 50 μs /phase current pulses are shown in Figure 3B.

The updates to the MVP architecture successfully encode acceleration to PFM pulse trains, shown in Figure 4. During translational movement, the rate modulated appropriately above and below a baseline of 100 pulses per second. During combined translational and rotational movement, both outputs modulated appropriately without evidence of cross-coupling.

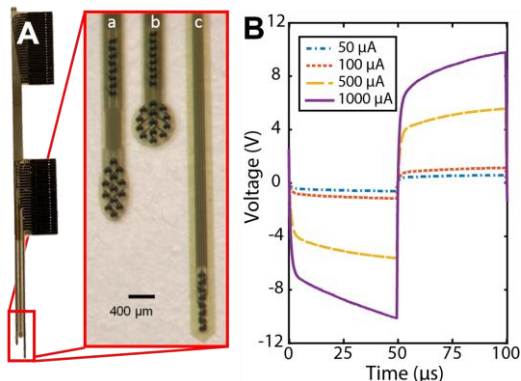


Figure 3. A. Polyimide electrode arrays. (a) shank intended for horizontal SCC and saccule; (b) shank for superior SCC and utricle; (c) shank for posterior canal. B. Voltage recordings during biphasic current driven stimulation using the new electrode arrays.

4 Interpretation

Based on the measured impedances of the new electrode arrays and the use of the MVP stimulation circuitry described in [7], with the compliance voltage at 12 V we can drive the new electrodes with charge-balanced, biphasic pulses up to 1 mA/phase of current. In previous work, this current range was sufficient for vestibular stimulation [4]. The increased number of electrodes and organized layout of the electrode contacts in the array provides greater control and increased capabilities for the stimulation paradigm, creating the ability to stimulate across the utricular/saccular surfaces.

With the results from the additions to the MVP architecture, we will be able to drive the PFM stimulation for the utricle and saccule to encode GIA. The addition of the

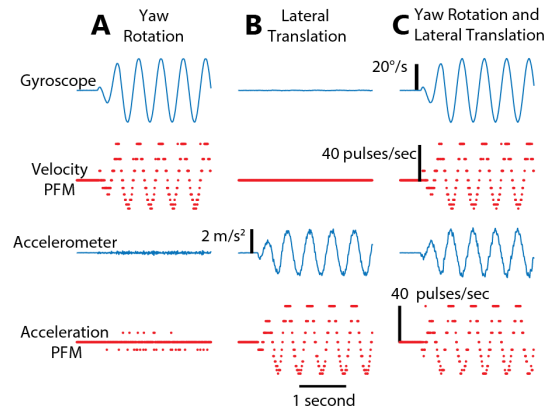


Figure 4. Instantaneous pulse frequency modulated (PFM) electrode output (red) and motion sensor signals (blue) during A. yaw rotation, B. lateral translation, C. simultaneous yaw and lateral movements.

necessary hardware and firmware provides a means to sense and encode linear accelerations and changes in head orientation with respect to gravity. The MVP system is capable of delivering stimulation via any of the 50 electrode contacts that the new electrode arrays offer. With these improvements to the design of the MVP system, we begin to move toward restoration of GIA sensation.

Supported by NIDCD (R01DC009255). Polyimide microelectrode arrays were designed and fabricated with funding from NIDCD contract Y1-DC-8002-01 and under the auspices of the U.S. Department of Energy by the Lawrence Livermore National Laboratory, Contract number DE-AC52-07NA27344.

References

- [1] D.Q. Sun, B.K. Ward, Y.R. Semenov, J.P. Carey, and C.C. Della Santina, “Bilateral Vestibular Deficiency,” *JAMA Otolaryngol. Neck Surg.*, vol. 140, no. 6, pp. 527–534, 2014.
- [2] G. Y. Fridman and C. C. Della Santina, “Progress Toward Development of a Multichannel Vestibular Prosthesis for Treatment of Bilateral Vestibular Deficiency,” *Anat. Rec. Adv. Integr. Anat. Evol. Biol.*, vol. 295, no. 11, pp. 2010–2029, Nov. 2012.
- [3] W. Gong and D. M. Merfeld, “System design and performance of a unilateral horizontal semicircular canal prosthesis,” *IEEE Trans. Biomed. Eng.*, vol. 49, no. 2, pp. 175–181, 2002.
- [4] C.C. Della Santina, A. Migliaccio, and A.H. Patel, “A multichannel semicircular canal neural prosthesis using electrical stimulation to restore 3-D vestibular sensation,” *IEEE Trans. Biomed. Eng.*, vol. 54, no. 6, pp. 1016–30, Jun. 2007.
- [5] B. Chiang, G. Y. Fridman, D. Chenkai, M.A. Rahman, and C.C. Della Santina, “Design and performance of a multichannel vestibular prosthesis that restores semicircular canal sensation in rhesus monkey,” *IEEE Trans. Neural Syst. Rehabil. Eng.*, vol. 19, no. 5, pp. 588–598, Oct. 2011.
- [6] K. Nie, L. Ling, S. M. Bierer, C. R. S. Kaneko, A. F. Fuchs, T. Oxford, J. T. Rubinstein, and J. O. Phillips, “An Experimental Vestibular Neural Prosthesis: Design and Preliminary Results with Rhesus Monkeys Stimulated with Modulated Pulses,” *IEEE Trans. Biomed. Eng.*, vol. 60, no. 6, pp. 1685–1692, 2013.
- [7] K.N. Hageman, Z.K. Kalayjian, F. Tejada, B. Chiang, M.A. Rahman, G. Y. Fridman, C. Dai, P. O. Pouliquen, J. Georgiou, C.C. Della Santina, and A.G. Andreou, “A CMOS Neural Interface for a Multichannel Vestibular Prosthesis,” *IEEE Trans. Biomed. Circuits Syst.*, IEEE Early Access, May 2015.
- [8] R. Hayden, S. Sawyer, E. Frey, S. Mori, A. a Migliaccio, and C. C. Della Santina, “Virtual labyrinth model of vestibular afferent excitation via implanted electrodes: validation and application to design of a multichannel vestibular prosthesis,” *Exp. Brain Res.*, vol. 210, pp. 623–40, May 2011.
- [9] L. S. Robblee and T. L. Rose, “Electrochemical Guidelines for Selection of Protocols and Electrode Materials for Neural Stimulation,” in *Neural Prostheses: Fundamental Studies*, W. F. Agnew and D. B. McCreery, Eds. Englewood Cliffs, NJ: Prentice Hall, 1990, pp. 26–66.
- [10] J. M. Goldberg, G. Desmadryl, R. a Baird, and C. Fernández, “The vestibular nerve of the chinchilla. IV. Discharge properties of utricular afferents,” *J. Neurophysiol.*, vol. 63, no. 4, pp. 781–790, 1990.
- [11] S. S. Desai, C. Zeh, and A. Lysakowski, “Comparative morphology of rodent vestibular periphery. I. Saccular and Utricular Maculae,” *J. Neurophysiol.*, vol. 93, pp. 251–266, 2005.